Energy Economics 80 (2019) 434–451

Contents lists available at ScienceDirect

Energy Economics

journal homepage: www.elsevier.com/locate/eneeco

Effect of Climate Change on wind speed and its impact on optimal power system expansion planning: The case of Chile

Catalina Rosende [a], Enzo Sauma [a,*], Gareth P. Harrison [b]

[a] Industrial and Systems Engineering Department and UC Energy Research Center, Pontificia Universidad Católica de Chile, Chile
[b] School of Engineering, The University of Edinburgh, Edinburgh, UK

ARTICLE INFO

Article history:
Received 22 September 2017
Received in revised form 4 January 2019
Accepted 17 January 2019
Available online 29 January 2019

JEL classification:
L11
L94
Q42
Q54

Keywords:
Climate Change
Power system economics
Power system expansion planning
Wind power generation

ABSTRACT

This work assesses the changes in power capacity expansion decisions regarding power generation and transmission that occur when the effects of Climate Change on wind speed are captured in the decision model. Considering an 85-year period (2016–2101), we use a Mixed-Integer Linear Program (MILP) model to analyze the optimal power capacity expansion in diverse types of power generation technologies, throughout the years and geographical locations. The optimization model minimizes the total (investment and operational) costs of the power system subject to several technical and economic constraints. We implement our model using the main Chilean power system. We compare two scenarios: one assuming that Climate Change affects wind speeds and hence wind farm capacity factors and the other assuming it does not. Our results reveal that, when taking into account the impact of Climate Change on wind speed, the optimal power generation and transmission expansion plan is different than when ignoring this effect. The variation of wind speed affects not only wind power capacity installed, but also other-technology power capacity installed. In particular, power capacity installed in wind and solar generation plants is higher (measured in MW installed) than the power capacity installed when we ignore the effects of Climate Change; and power capacity installed in diesel and natural gas technologies are lower. We perform sensitivity analyses, changing power capacity expansion limits and the discount rate, to check for the robustness of our results.

1. Introduction

Climate Change awareness has increased worldwide. Scientists (IPCC, 2000, 2013) have studied how to mitigate Climate Change and how to be prepared for the changes. In the power sector, scholars (Garreaud, 2011; Harrison et al., 2008; Sailor et al., 2008) have studied how changes in the climate could affect energy development, especially considering renewable energy sources (RES) technologies for power generation.

From a planning and operational perspective, one of the most challenging aspects of wind power is its variability (Cradden et al., 2012). Changes in wind speed, within the interval from 6 m/s to 10 m/s, may be the difference between a profitable or a non-profitable wind power plant (Harrison et al., 2008). Thus, estimating wind variability and considering these estimations in the evaluation of energy projects is crucial, especially in this Climate Change era.

The main purpose of this work is the analysis of the changes in expansion decisions regarding power generation and transmission that occur when the effects of Climate Change on wind speed are captured in the decision model. Considering an 85-year period (2016–2101), we use a Mixed-Integer Linear Program (MILP) model to analyze the optimal power capacity installed in diverse types of power generation technologies, throughout the years and geographical locations. In particular, we consider the changes in technology, magnitude, location, and timing of power transmission and generation capacity expansion. In doing this, we consider two scenarios. The first one assumes that the capacity factors of RES wind power plants may be critically affected by Climate Change. It therefore incorporates the effects of Climate Change on wind speed. The second scenario assumes that these capacity factors stay constant. Simulation outcomes of both cases are compared in the case of the main Chilean network to assess differences regarding capacity expansion in power generation and transmission.

Some authors (Munoz et al., 2017) have studied how Climate Change affects hydropower production, but they generally ignore the effects on wind power or the correlations among the impacts. Accordingly, before analyzing the impact of Climate Change on wind power production, it is necessary to explore the correlations among the power production for different RES technologies. In doing this analysis, we examine correlations among power generation of diverse types of RES technologies, using three years of hourly generation data from solar, hydroelectric (reservoir and run-of-river) and wind energy generators located in the North, Center and South of Chile. We then

* Corresponding author.
E-mail address: esauma@ing.puc.cl (E. Sauma).

https://doi.org/10.1016/j.eneco.2019.01.012
0140-9883/

use inter-seasonal and inter-hour measures of wind speeds to study how wind capacity factors may change in different scenarios of greenhouse gas emissions in different years. Finally, we use all this information to assess the changes in the optimal power system expansion plan when considering and ignoring the effects of Climate Change on wind speed.

The rest of this article is organized as follows. Section 2 describes correlations between power generation of different RES (i.e., wind, run-of-river hydro, reservoir hydro, and solar). Section 3 discusses the evolution of wind speed in different scenarios of greenhouse gas emissions and shows a spatial and temporal analysis of changes in the wind speed in different cases. Section 4 presents an optimization model for the expansion of the electrical system in Chile for two cases: one that includes alterations in wind speed due to Climate Change and another that assumes constant capacity factors for wind power generation. Section 5 explains the data we used for the model implementation in the case of the main Chilean network. Section 6 shows the simulation results and their discussion. In this section, we also perform sensitivity analyses to check for the robustness of the results. Section 7 concludes the paper.

2. Correlations among RES productions in Chile

One of the many countries that have become progressively aware of environmental issues is Chile. The country must satisfy the increasing demand of energy, while complying with the conditions of a developed country. According to the Ministry of Energy, electricity consumption between 1990 and 2013 grew by 319.1% (CDEC-SIC, 2015). An average annual increase of 2.7% in energy demand is predicted until 2025, and 2% thereafter (CDEC-SIC, 2017). Chile has one of the highest per capita carbon dioxide emission rates among countries in Latin America and the Mercosur (Mundaca, 2012). It faces the challenge of creating an effective and ambitious power capacity expansion, through diverse generation technologies, including RES such as wind, solar, and hydro power.

At the global level, wind power has led recent RES investments to mitigate Climate Change. Wind now commands a significant share of the world's electricity supply (global capacity stood at around 350 GW at the start of 2015 and is rising at 35% per year). Wind now comprises 13% of installed capacity in Europe (a greater share than nuclear power), and can provide more than the entire national load in five countries, including Germany and Spain (Staffell and Pfenninger, 2016).

Given its topography (mountains, valleys, and coasts), Chile may well be considered the country with the second highest wind potential in South America and the Caribbean, estimated at 40,000 MW of installable capacity (Santana, 2014). Some authors have stated that the best future wind projects in Chile could achieve an average capacity factor of 37.9%. In the worst scenario, it would reach a factor of 25.2% (Watts et al., 2016), a good prospect for wind generation. Watts and Jara (2010) have suggested that a viable option to reduce carbon emissions in the northern area of Chile is to encourage wind power generation. In addition, Garreaud and Falvey (2008) argue that coastal wind speeds in Chile will increase by 15% toward the end of the century, allowing more onshore and offshore wind projects to become feasible.

On the other hand, in a country as long and narrow as Chile (2.653 miles long and an average of 110 miles wide–from the Andes to the Pacific Ocean), in which different atmospheric conditions jointly occur, it is ambiguous whether RES generators along Chile could complement each other in diverse weather conditions.

In this section, we analyze the correlations among the power produced by solar, hydroelectric (reservoir and run-of-river) and wind power plants located in the Northern, Central and Southern parts of Chile. We use real-measured data from August 2013 to July 2016. The aim of this exercise is to check that correlations are not significant in the same block time and season, meaning that independent analyses of the effect of Climate Change on wind, hydro and solar generation are needed when analyzing the power system expansion planning.

The Chilean National Electric Coordinator provides data for most RES generators in Chile. This institution coordinates the operation of the power installations at the generation and transmission levels. The data include hourly power generation (for the three years mentioned before) from wind, reservoir hydro, run-of-river hydro, and solar power plants throughout Chile. We aggregated the data into 10 groups, according to RES technology and zone (i.e., Run-of-river North/Center/South, Reservoir Center/South, Wind North/Center/South, Solar North/Center). There is no reservoir hydropower generation in the North of Chile (where the dry, arid desert is located) and no solar energy generation in the South region (where solar radiation is limited and there is a short summer season).

Data were analyzed on a per-semester basis, considering "summer" periods (from October to March) and "winter" periods (from April to September). We studied three summer period 2013/14, 2014/2015 and 2015/2016. We also consider three winter periods, which were built including data from August and September of the previous year in the winter period starting in April, in order to consider all the information contained in the available data.[1]

For every semester, correlations are calculated using hourly data. Fig. 1 graphically shows the correlation levels in the case of the three winter periods studied. On the right side of every matrix, there is a color scale representing the level of the corresponding correlation value. We use the same scale in all matrices. The size of each dot in the matrix depends on the absolute value of the correlation between two specific RES-zone combinations.

Correlation results for the first winter period are shown in the upper matrix. A surprisingly high positive correlation is observed between solar generation in the North zone and run-of-river hydro generation in the same zone. This suggests that solar intensity and run-of-river intensity may be related. A partial explanation is that intense sunshine melts the snow in the Andes Mountains, increasing the flow in the rivers. However, there is little snow in the mountains of the north of Chile. Rain is very scarce in the north too (e.g., considering the 900 miles between Arica and La Serena, the total rainfall in 2016 was 10.9 mm; DGAC Chile, 2016), making correlations insufficiently representative. In this upper matrix, we also observe a few minor negative correlations, as well as some slightly positive correlations, particularly between same zones and between reservoir hydro and run-of-river hydro.

Results for the second winter period analyzed are presented in the middle matrix of Fig. 1. Again, there is a high positive correlation between solar generation in the North and run-of-river hydro generation in the North. We also observe a positive correlation between the energy generated by reservoir and run-of-river hydro power in the central zone, which makes sense due to the influence of rain patterns. Regarding wind power plants, in this period we observe that wind generation in the North is positively correlated both with run-of-river generation and with solar generation; while wind generation in the Center is negatively correlated both with run-of-river generation and reservoir hydro generation. This is partially explained by the fact that, in the central part of Chile, wind usually comes before rain and not while raining.

The lower matrix of Fig. 1 shows correlation results for the third winter period studied (April to July of 2016 plus August and September of 2015). Several hydro plants are positively correlated to each other. There are no high negative correlations in this period. Wind generation in the South is positively correlated with wind generation in the Center; and solar generation in the North is positively correlated with solar generation in the Center. We also observe that the previously-observed positive correlation between solar generation in the North zone and run-of-river hydro generation in the same zone totally disappears.

[1] In order to include all the information contained in the available data (August 2013–July 2016), we included data for period August 2013 and September 2013 in the winter period starting in April 2014. Hence, the first winter period studied has information measured from April 2014 to July 2014 plus August 2013 and September 2013. The two other winter periods were built in the same manner.

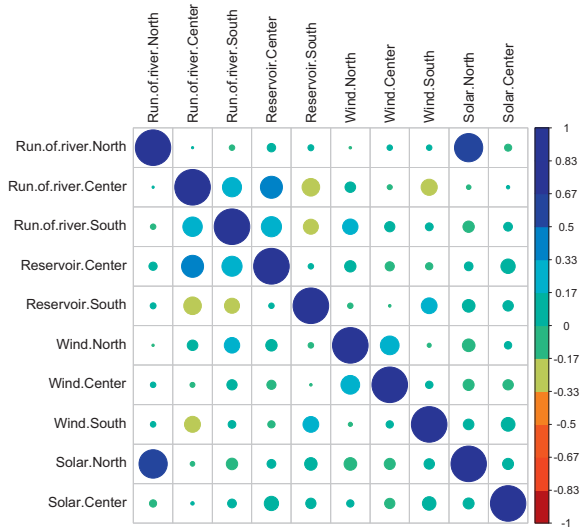

Correlations among hourly generation from April to October 2013-2014

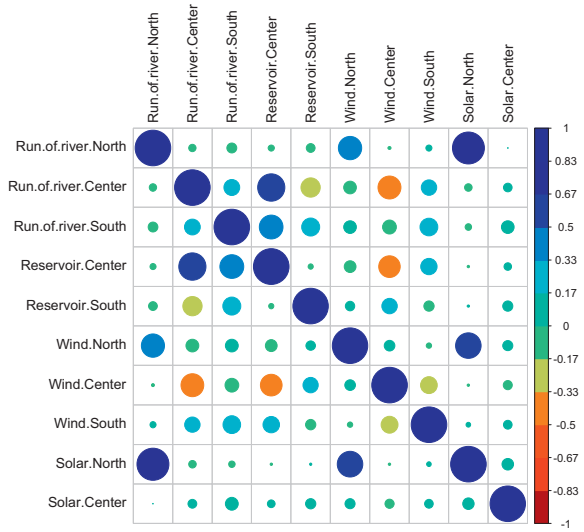

Correlations among hourly generation from April to October 2014-2015

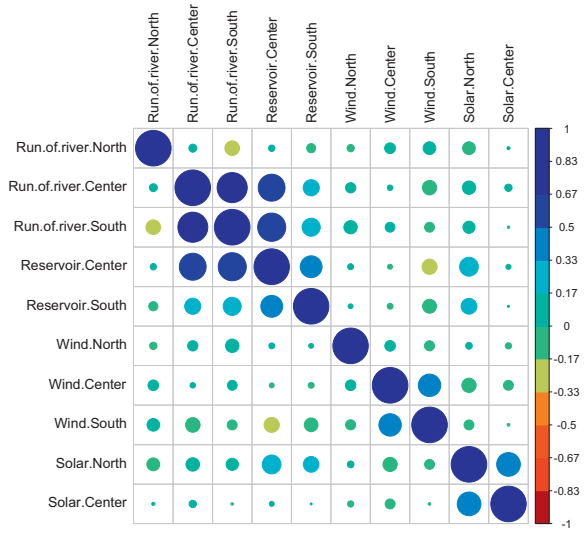

Correlations among hourly generation from April to October 2015-2016

Fig. 1. Correlations of hourly power generation among RES types in Winter periods.

Summarizing results in these three winter periods, the only recurring correlations are among hydro sources.[2] Regarding other correlations, in two of the three winter periods, positive correlations are found in the North zone between solar and run-of-river hydro generation. Generally speaking, there is no strong pattern that would suggest the existence of a relationship among the different types of RES generation.

Summer periods' results are shown in Fig. 2. The upper matrix shows correlation results considering the hourly generation registered between October of 2013 and March of 2014. During this period, solar generation is included only in the North zone because it was zero in the other regions. As in winter periods, there are slight positive correlations among hydro generation technologies. Results also suggest a negative correlation in the South between wind generation and run-of-river hydro generation, meaning that wind is strong when rainfall is scarce, and vice versa.[3] In the North zone, there is a positive correlation between solar and run-of-river hydro generation. A partial explanation is that, as mentioned before, intense sunshine melts the snow in the Andes Mountains. However, it is also important to highlight that the extreme scarcity of rain in the north of Chile may also explain these results.

The middle matrix of Fig. 2 describes correlations for the period from October of 2014 to March of 2015. Again, there is a strong positive correlation between solar and run-of-river hydro generation in the North. There is also a slightly positive correlation between run-of-river hydro generation in the South and reservoir hydro in the central part of Chile.

The bottom matrix of Fig. 2 illustrates correlations obtained with data from October of 2015 to March of 2016. As in the other periods, generation from diverse hydro plants is correlated. There are other positive correlations, particularly between solar generation in the North and in the Center.

Succinctly, the three summer periods analyzed do not show a strong pattern that would suggest that wind generation is correlated with power from other RES technologies.

Therefore, considering the results in winter and summer periods, we cannot observe evidence of a correlation between wind power generation and power production from other RES. Accordingly, we can argue that the impact of Climate Change on wind power production can credibly be studied independently from its impact on other RES.

3. Projected wind speed evolution under different scenarios of greenhouse gas concentrations

In this section, we present an analysis of the expected changes in wind speed in Chile for the coming decades. The data was provided by the National Center for Atmospheric Research (NCAR, 2017).[4]

We study future wind speed evolutions for different timing and locations along Chile. The specific locations are chosen according to the nodes that the Chilean Ministry of Energy has established in its long-term strategic plan (PELP, from Spanish) as strategic power network points. The rationale for assuming this is that it is likely that power stations near these strategic points will have to pay relatively low transmission costs to inject their energy into the system, compared to power stations that are far from strategic nodes.

We report wind speed projections for the years 2030, 2050, and 2100, under different scenarios of greenhouse gas concentrations. These scenarios are called Representative Concentration Pathways (RCP). We consider three RCPs: RCP 4.5, RCP 6.0, and RCP 8.5. The first two are stable scenarios, respectively involving a CO_2 level of 528 parts per million (ppm) and 670 ppm by year 2100. The third scenario, RCP 8.5 represents a higher level of greenhouse gas emissions and involves a concentration of CO_2 of 936 ppm by year 2100 (IPCC, 2013).

To extract wind speed data from the NCAR database, we searched the data panel for the longitude and latitude of every location considered in this study. We extracted the wind speed data for four specific hours of the day (6:00, 12:00, 18:00, and 24:00; this is due to the availability of data from NCAR), for every day of the year, for every selected location, and for every RCP scenario. Then, using this information, we run a k-means clustering technique in R in order to group every set of wind speed data into 12 clusters of similar characteristics (i.e., wind speed levels). As a result, we obtained 12 clusters for each hour block of the day (i.e., for each hour within the 4 h with wind speed information), for each node (i.e., location), for each RCP scenario, and for each year considered. Then, for each cluster, we computed the average wind speed to be the representative wind speed of that cluster. The main idea behind the use of this k-means clustering technique is to obtain 12 representative days of the year selected, for each location and each RCP scenario (i.e., days with similar wind speed characteristics are within the same cluster). Nonetheless, it is worth to mention that the benefit of obtaining a good representation of the annual wind speed data comes also with the cost of losing the chronological order among clusters.

Accordingly, for each of the resulting representative days, we gathered the wind speed projections for the four specific hours of the day (6:00 12:00, 18:00, and 24:00), for years 2030, 2050, and 2100, in every selected node and RCP scenario. Wind projections in the database are made at 125 m from ground level.

The analyzed sites are 10 nodes of the *Sistema Interconectado del Norte Grande* (SING),[5] the interconnected system that serves the farthest northern area of Chile, and 19 nodes of the *Sistema Interconectado Central* (SIC),[6] the central interconnected system of Chile. These are the two largest power networks in Chile. Fig. 3 shows a graphical representation of the Chilean network considered in this work.

Fig. 4 contains Graphs 1–4, which show the average wind speeds for every group of nodes [SING, SIC(1), SIC(2), and SIC(3), respectively]. The different shapes reflect the scenarios, and the different colors reflect the observed years (2030, 2050, and 2100). Specifically, squares represent scenario RCP 4.5, circles RCP 6.0, and diamonds RCP 8.5. Colors represent years: orange refers to year 2030, blue to 2050, and green represents year 2100.

Graph 1 shows data for SING nodes. Comparing year-scenario combinations, wind speeds differ in >1 m/s in most nodes. The year-scenario combination that is projected to have the highest wind speed in most SING locations is the RCP 8.5 scenario in year 2050. In some areas, the highest projected wind speeds are found in the RCP 4.5 scenario, but also in year 2050. However, the second-best situation in terms of wind speed in those locations is in the RCP 8.5 scenario in year 2050. This combination of year, RCP, and location is favorable for wind generation and also for the environment due to a healthier air composition.

Graph 2 shows data for SIC(1), the northern segment of the central interconnected system. Here, in most SIC(1) locations, the highest wind speeds occur in the RCP 8.5 scenario in year 2050. There are two locations where the highest wind speeds occur in the RCP 6.0 scenario in year 2030.

Graph 3 shows that, in all SIC(2) locations, the highest wind speeds occur in the RCP 6.0 scenario in year 2030. Within this scenario, wind speeds will decrease by an average of 1.1 m/s from 2030 to 2100. In the case of the SIC(3) nodes, as shown in Graph 4, the difference between the best and the worst scenario in terms of wind speed, is 1.2 m/s in

[2] Naturally, there are some exceptions, which are related to the fact that, in general, run-of-river hydro plants are not able to choose the time for generation, while reservoir hydro plants make a strategic management of water, saving sometimes water to satisfy future demand.

[3] In the south of Chile, it is relatively common having strong winds in the hours or days before big rainfalls; and once the rain starts, the wind diminishes notably.

[4] This institution is a U.S. federally funded research and development center, managed by the nonprofit University Corporation for Atmospheric Research (UCAR) and funded by the National Science Foundation (NSF).

[5] The SING nodes are: Atacama, Changos, Collahuasi, Cóndores, Encuentro, Kimal, Laberinto, Lagunas, Parinacota and Tarapacá.

[6] For analytical convenience, we analyze the SIC nodes in three different groups, separating them mainly in a geographical way, from North to South. SIC(1) includes the nodes that are geographically in the northern part of the SIC system: Cardones, Cumbres, Las Palmas, Pan de Azúcar, Paposo and Punta Colorada. SIC(2) follows, with Alto Jahuel, Candelaria, Cerro Navia, Los Vilos, Polpaico and Rapel. SIC(3) includes the most southern area of the SIC system: Ancoa, Cautín, Chiloé, Mulchén, Puerto Montt, Rahue and Valdivia.

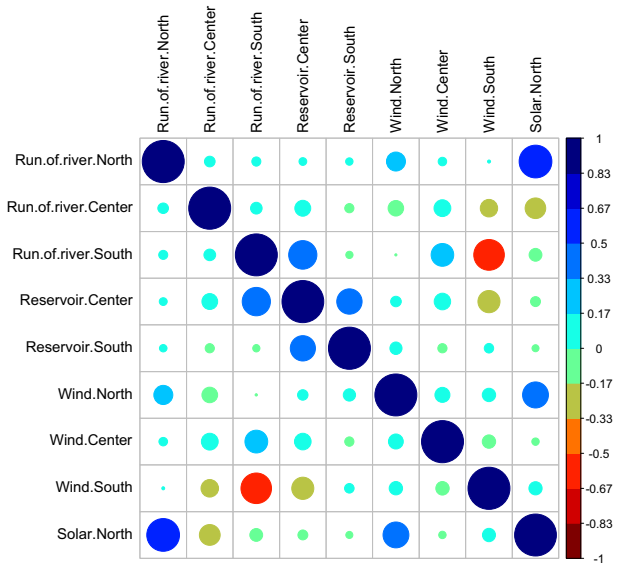

Correlations among hourly generation from October to April 2013-2014

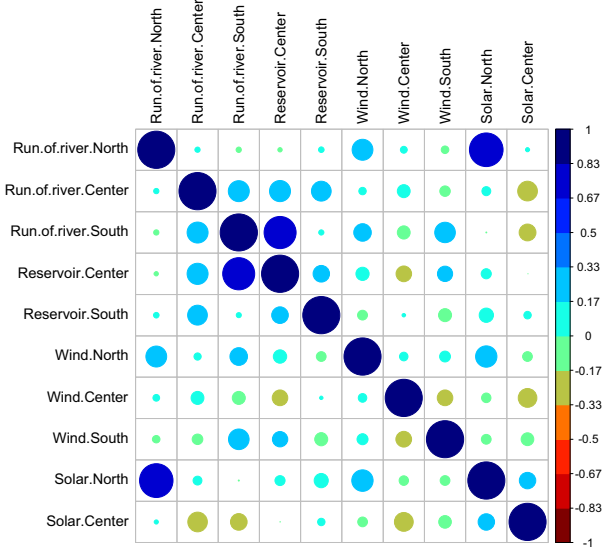

Correlations among hourly generation from October to April 2014-2015

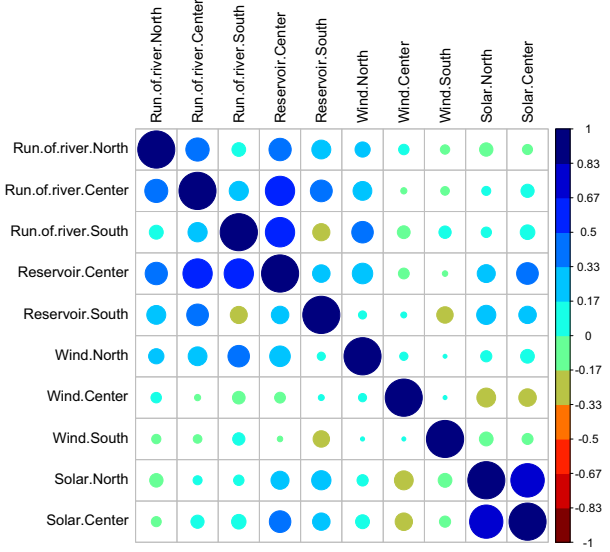

Correlations among hourly generation from October to April 2015-2016

Fig. 2. Correlations of hourly power generation among RES types in Summer periods.

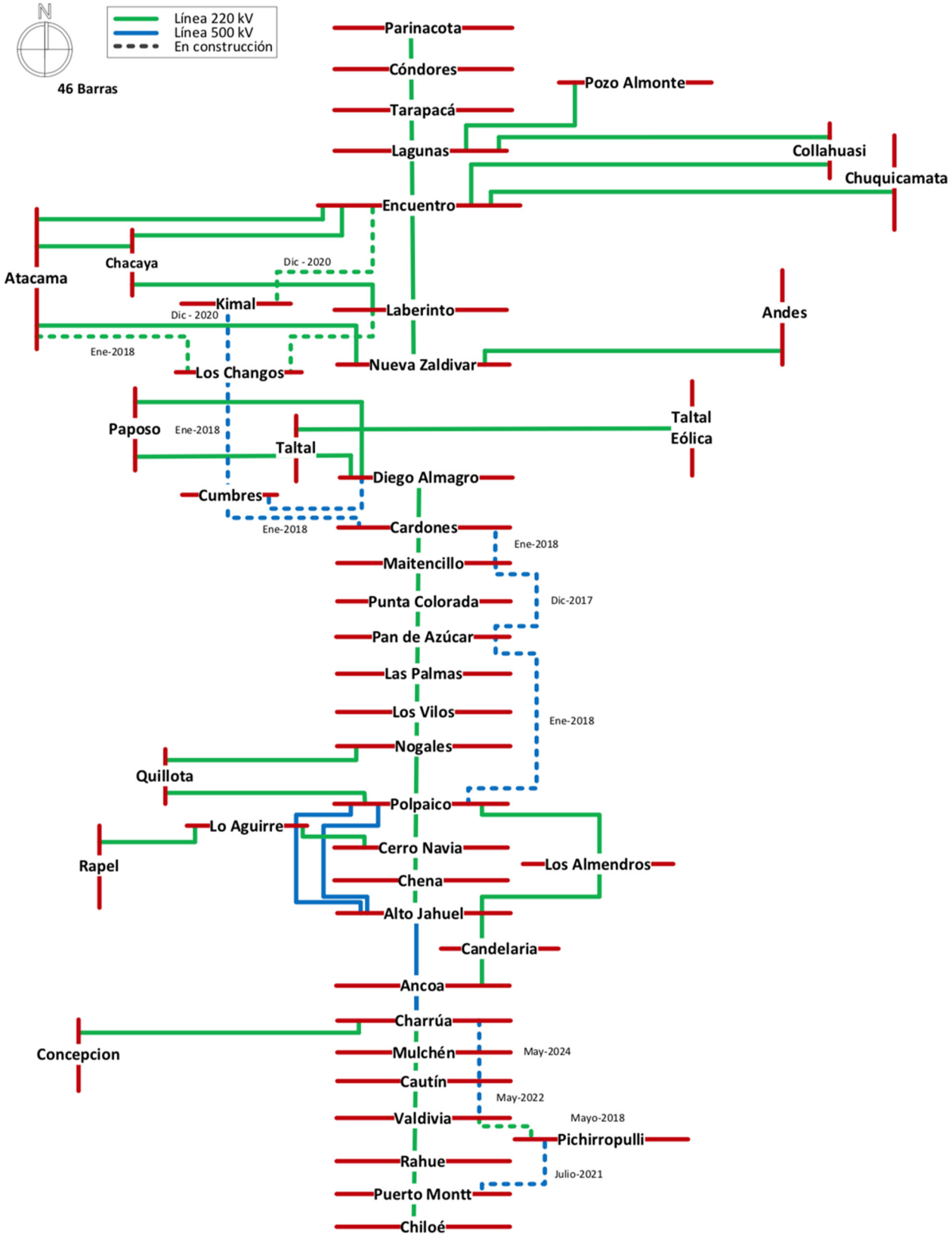

Fig. 3. Representation of the Chilean network considered.

average. Changes in wind speed affect the capacity factor, the stability and the effectiveness of generation, which adds vulnerability to the system. In scenarios RCP 4.5 and RCP 8.5, wind speeds are in general more stable along the years. This imparts more stability to the system as well.

To clearly appreciate the effects that changes in RCP perpetrate in different scenarios, we repeated the previous analyses, this time keeping the year constant (specifically year 2030) and changing only gas concentrations. SIC nodes were segmented with the same criteria

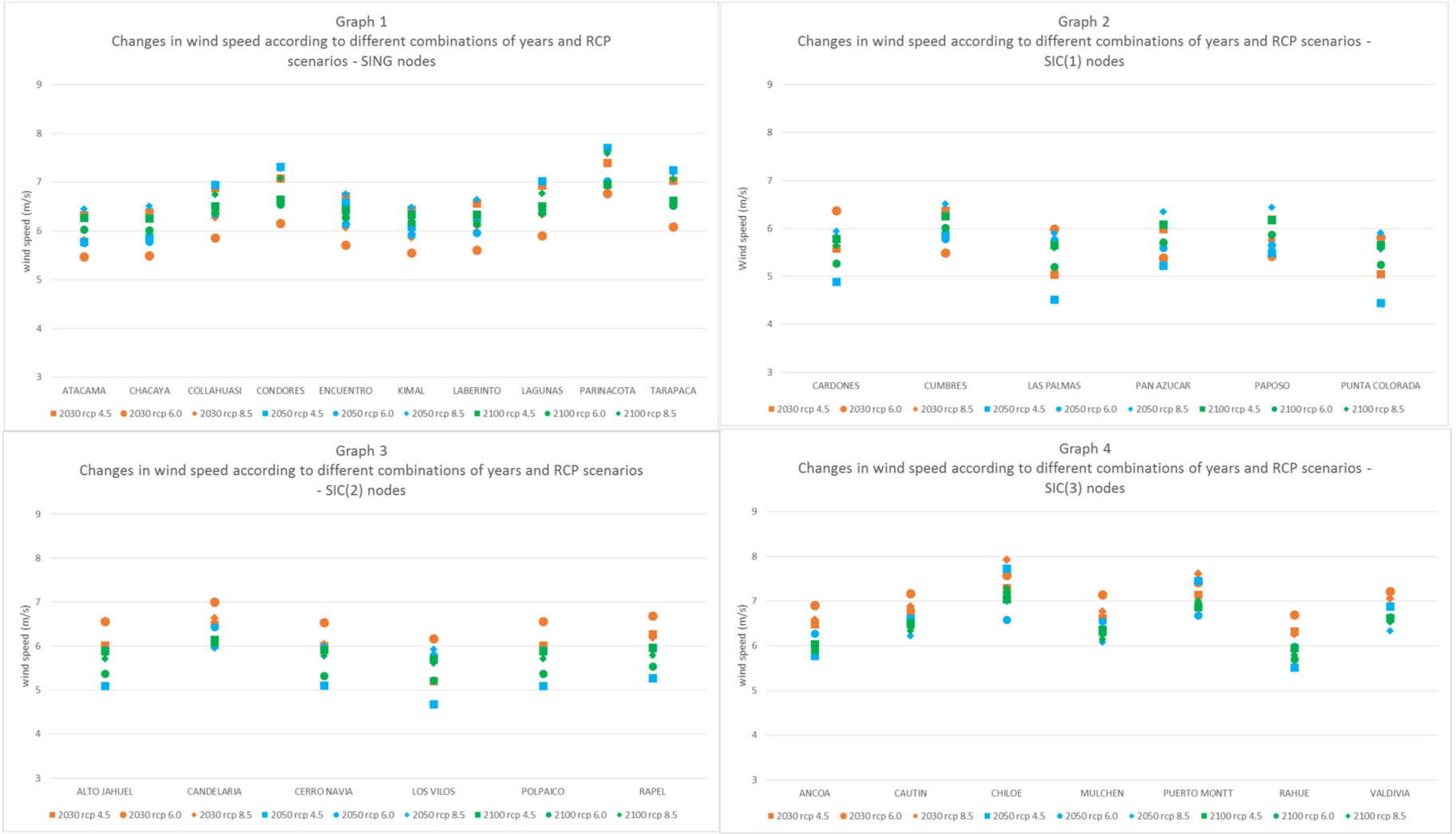

Fig. 4. Changes in wind speed according to different combinations of years and RCP scenarios. (For interpretation of the references to color in this figure, the reader is referred to the web version of this article.)

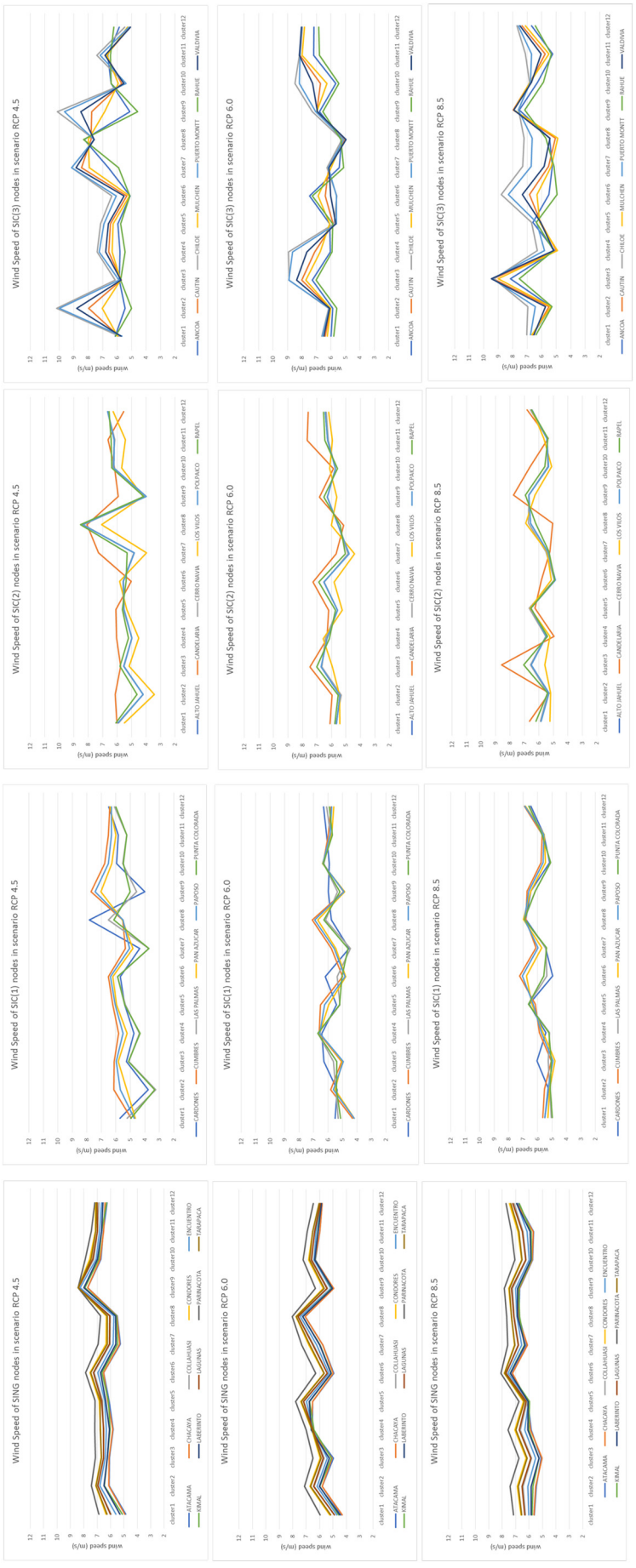

Fig. 5. Wind speed in different RCP scenarios.

as above. Hence, there are four groups of nodes and 3 scenarios for each group; consequently 12 graphs. Fig. 5 displays these graphs in three rows and four columns. Every row contains a different RCP scenario (e.g., the top row displays four graphs for RCP 4.5) and every column represents a different group of nodes [SING, SIC(1), SIC(2), and SIC (3)]. The first column in Fig. 5 shows results for the SING nodes within year 2030. Roughly speaking, wind speed slows down if RCP is 6.0 instead of 4.5. This holds for almost all nodes in this group. The speed vary between −0.9 m/s to 1.8 m/s between these two scenarios. If RCP is 8.5 instead of 6.0, wind speeds increase again, reaching similar values than in RCP 4.5. The average annual wind speed for all the scenarios and block times in the SING area is 6.74 m/s.

The second column in Fig. 5 displays three graphs (one for each RCP) for wind speeds in the SIC(1) nodes. There are some significant changes in wind speed among scenarios. Amidst different RCP scenarios, the annual average wind speed for all SIC(1) nodes has maximum variations of about 1 m/s. The biggest change occurs in Cumbres, where the annual average speed moves from 6.4 m/s in RCP 4.5 to 5.2 m/s, in RCP 6.0 This implies that a rise in greenhouse gases could bring a decrease in wind speeds of 1.2 m/s in the Cumbres area. In 2030, the total average speed in SIC(1), considering all scenarios and months, is 5.8 m/s.

Repeating the above analysis for the SIC(2) nodes, displayed in the three graphs standing in the third column of the same figure, we observe that average annual wind speeds slightly increase when moving from the RCP 4.5 scenario to RCP 6.0, and when moving from the RCP 6.0 scenario to RCP 8.5. As in the case of the SIC(1) nodes, there are significant changes in wind speed among scenarios in some locations. In Los Vilos, for instance, the average wind speed increases 0.8 m/s between RCP 4.5 and RCP 8.5. In average, the change in wind speed is about 0.7 m/s among scenarios.

The last column of graphs in this figure displays data from the southern nodes, SIC(3). Between the scenario RCP 4.5 and RCP 6.0 the wind speed slightly decrease in the nodes of this group. Specifically, between these scenarios the wind speed changes 0.25 m/s in average. With respect to scenario RCP 8.5, average wind speeds increase again to similar levels than in the RCP 4.5 scenario.

Of all the zones analyzed, the ones with the highest wind speeds, regardless of the gas concentration scenario, are almost always found in the SING areas. Every analyzed place in the SING is projected to have average annual speeds higher than 6.2 m/s. This confirms the idea that wind generation in the North will have good results in almost all areas and scenarios (Watts and Jara, 2010).

As for specific zones throughout Chile, the highest average speeds, regardless of the greenhouse gas scenarios, are in Parinacota (with an average of 7.4 m/s), the southern island Chiloé (7.2 m/s), Puerto Montt (6.9 m/s), Cóndores (6.8 m/s), Collahuasi (6.8 m/s), Tarapacá (6.7 m/s), and Lagunas (6.6 m/s). These average speeds would allow wind generation with an average capacity factor higher than 20%.

For every location and for each of the specified years (2030, 2050, and 2100), we calculate wind speed averages for the three analyzed RCP scenarios (RCP 4.5, 6.0, and 8.5). Fig. 6 displays these averages for every node for years 2030, 2050 and 2100. Every column is a different group of nodes and every row is a different year. In the first column, which represents averages for the SING system, it is noteworthy that between 2030 and 2050 speed changes by less than ±0.4 m/s for all nodes. From 2050 to 2100 speeds also rise at every point (by <0.2 m/s). Hence, speeds in the farthest northern area of Chile are expected to be relatively stable. The annual averages for the SING nodes (first column of graphs in Fig. 6) are 6.2 m/s in 2030, 6.4 m/s in 2050, and 6.5 m/s in 2100. The SING zones with the highest average speed for the three analyzed periods are Parinacota, with an average speed of 7.1 m/s, and Cóndores, with an average of 6.8 m/s. In column 2 [SIC(1) nodes], the speeds remain fairly constant over the years. The annual average for each year in the SIC(1) areas is 5.6 m/s in 2030, 5.8 m/s in 2050 and 5.9 m/s in 2100. Of the nodes in this set, the only ones with an average speed of 6 m/s or more are Cumbres, Pan de Azucar and Paposo. Column 3, [SIC(2) nodes], shows a decrease in average wind speed over the years. The annual average for each year in the SIC(2) areas is 6.1 m/s in 2030, 5.8 m/s in 2050 and 5.4 m/s in 2100. The only location within these nodes with an average wind speed higher than of 6 m/s is Candelaria. Column 4 exhibits data for SIC(3), the southern zone of Chile. As in the case of SIC(2) nodes, average wind speeds decrease over the years in most locations. The annual average for each year in the SIC(3) areas is 6.6 m/s in 2030, 6.2 m/s in 2050 and 5.7 m/s in 2100. Chiloé and Puerto Montt are the locations with the highest average wind speeds (around 7 m/s in average).

For illustration purposes, Fig. 7 shows wind speed variations under different RCP scenarios for Cóndores, one specific area in the North of Chile with high wind speed projections.

From Fig. 7, we can observe that, in some cases, there are >4 m/s difference among scenarios. This can significantly change the capacity factors of a wind power plant. In general, for the year 2050 and 2100 the highest speeds are in the worst scenario: RCP 8.5. In 2030 the highest speeds are in the best scenario: RCP 4.5. However, as Fig. 7 shows, there are large differences of wind speeds among the diverse combinations of cases and years.

The analyzed data invites deeper analysis regarding the convenience of installing a large number of wind power plants in the north of Chile and in the southern island Chiloé. On the other hand, it is necessary to study the actions that are being taken not only in Chile, but in the rest of the world, to have accurate forecasts of RCP scenarios, thus being able to make more informed decisions regarding the places where to install wind power plants to maximize energy generation.

4. Optimization model for the system expansion planning of the electrical system in Chile

In this section, we formulate an expansion planning model for the Chilean electrical system. The model is based on the formulation proposed by Munoz et al. (2013). As in (Munoz et al., 2013), our model minimizes total costs, composed of investment costs in power plants, transmission investment costs, and operational generation costs; subject to technical constraints (e.g., Kirchhoff's Current Law and Kirchhoff's Voltage Law). Differently than in (Munoz et al., 2013), our model allows for power plants with capacity factors that vary over time. In the case of Chile, recent work suggests that wind speeds are expected to change favorably in many areas –due to Climate Change– hence augmenting capacity factors (Barton, 2013; Sailor et al., 2008). Another difference of our model is that, considering the economic power capacity expansion possibilities of Chile, we set power capacity expansion limits for each generation technology. We also account for changes over time in energy demand.

In this setting, the optimization question is how to satisfy the increasing Chilean energy demand, while minimizing costs. With data of the expected demand and capacity factors for wind from 2016 to 2101, we run the model to identify the optimal timing and locations in which capacity expansion in transmission lines and in new power plants would result most cost-effective. The model is allowed to make capacity expansion decisions every five years between 2016 and 2101.

We compare two cases. Case 1 takes wind speed projections predicted by the National Center for Atmospheric Research (NCAR, 2017) and uses the Rayleigh distribution (Harrison et al., 2008) to transform the speeds into capacity factors, assuming turbines of 3 MW of rated power with a diameter of 45 m and a hub height of 100 m. In this way, we incorporate the possible effects of Climate Change on wind speed in different zones of Chile, in different years, and on various hours of the day. We assume constant capacity factors in all other generation technologies. Case 2 assumes that Climate Change does not affect the speed or intensity of winds in Chile; ergo, all capacity factors remain constant –at their 2016 levels- throughout the periods considered.

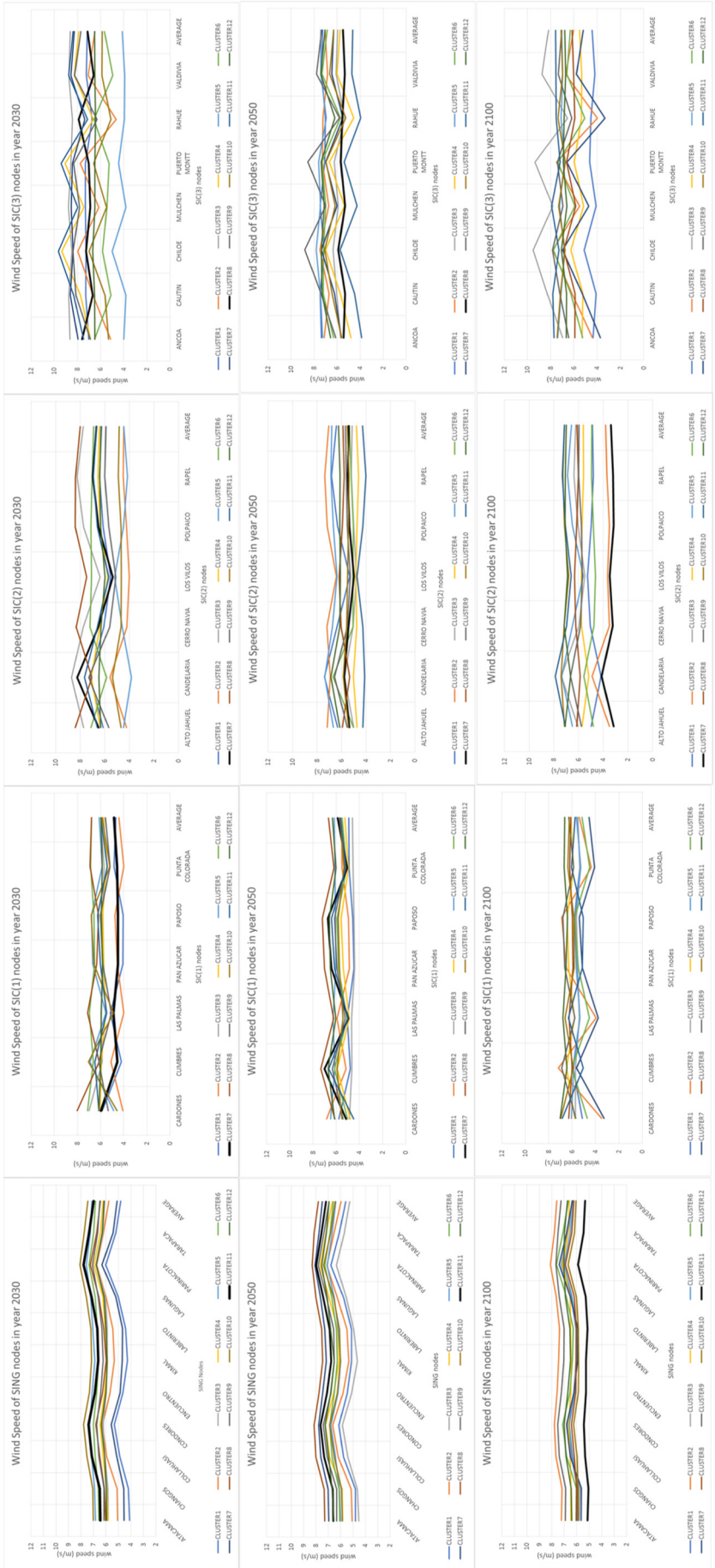

Fig. 6. Wind speed in different years and places.

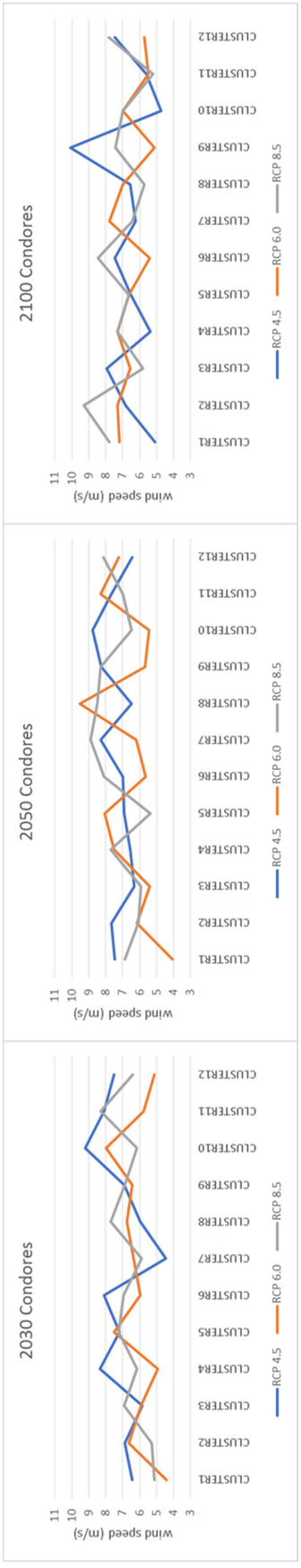

Fig. 7. Wind speed in Cóndores in different years.

Specifically, the model minimizes total system (investment and operating) costs, subject to a series of constraints: generation limits, nodal energy balances (DC approximation of Kirchhoff's Current Law), maximum power flow constraints, transmission line constraints (DC approximation of Kirchhoff's Voltage Law), and power capacity expansion limits per technology per period. We ignore transmission losses as well as the possibility of energy curtailment. Marginal costs of wind farms, as well as of solar and run-of-river hydro plants, are assumed to be zero. The model is formulated as follows.

$$Min \sum_{t\in T}\sum_{b\in B}\sum_{k\in K} CI_{b,k}y_{b,k,t}\delta^t + \sum_{t\in T}\sum_{l\in L}\sum_{s\in S} CC_l x_{l,s,t}\delta^t + \sum_{t\in T}\sum_{h\in H}\sum_{b\in B}\sum_{k\in K} MC_{b,k}g_{b,k,h,t}\delta^t \quad (1)$$

Subject to:

$$\sum_{t\in T} y_{b,k,t} \le Y^M_{b,k} \quad \forall b,k \quad (2)$$

$$\sum_{l\in L}\sum_{n\in S\cup C} f_{l,n,h,t} + \sum_{k\in K} g_{b,k,h,t} = D_{b,h,t} \quad \forall b,h,t \quad (3)$$

$$f_{l,c,h,t} - \gamma_l(\theta_{b,h,t} - \theta_{p,h,t}) = 0 \quad \forall b,p\in\Omega_l \quad \forall c\in C \quad \forall l,h,t \quad (4)$$

$$\left|f_{l,s,h,t} - \gamma_l(\theta_{b,h,t} - \theta_{p,h,t})\right| \le M\left(1 - \sum_{\tau\le t} x_{l,n,\tau}\right) \quad \forall (b,p)\in\Omega_l \quad \forall s\in S \quad \forall l,h,t \quad (5)$$

$$\left|f_{l,c,h,t}\right| \le F_{l,c} \quad \forall c\in C \quad \forall l,h,t \quad (6)$$

$$\left|f_{l,s,h,t}\right| \le F_{l,c}\sum_{\tau\le t} x_{l,n,\tau} \quad \forall s\in S \quad \forall l,h,t \quad (7)$$

$$g_{b,k,h,t} \le W_{b,k,h,t}\left(Y^0_{b,k} + \sum_{\tau\le t} y_{b,k,t}\right) \quad \forall b,k,h,t \quad (8)$$

$$\sum_{\tau\le t} x_{l,s,\tau} \le 1 \quad \forall l,s,t \quad (9)$$

$$\sum_{q\in Q}\sum_{h\in H}\sum_{b\in B} g_{b,q,h,t} \ge \alpha \sum_{k\in K}\sum_{h\in H}\sum_{b\in B} g_{b,k,h,t} \quad \forall t\in T \quad (10)$$

$$\sum_{b\in B} y_{b,k,t} \le IL_{t,k} \quad \forall t,k \quad (11)$$

$$\left|\theta_{b,h,t}\right| \le \frac{\pi}{2} \quad (12)$$

$$y_{b,k,t} \ge 0 \quad g_{b,k,h,t} \ge 0 \quad x_{l,s,t} \in \{0,1\} \quad (13)$$

The notation used here is explained next. B denotes the set of buses (or nodes, indexed by b), K the set of generation technologies (indexed by k), Q the subset of K consisting of renewable generation technologies (indexed by q), and L the set of lines (indexed by l). Ω_l represents the set (pair) of nodes connecting corridor l; C the set of circuits already built between one node and another (indexed by c); and S the set of candidate circuits to be built between two nodes (indexed by s). Indexed by n is the union of S and C. H is the set of hours per year (indexed by h), and t is the period that is being analyzed [with $t = ((\text{Year} - 2016)/5 + 1)$; hence $t = 3$ is year 2026, the third period evaluated, preceded by year 2021 ($t = 2$)]. M is a big positive number.

The main decision variables of the model are $y_{b,k,t}$ (in MW) representing new power capacity installed, $x_{l,s,t}$ (dimensionless 0–1 variable) for transmission capacity installed, and $g_{b,k,h,t}$ MW for generation; $f_{l,n,h,a}$ denotes the power flow (in MW) over corridor l and circuit n; $\theta_{b,h,a}$ (in radians) corresponds to the voltage phase-angle at bus b.

With respect to the parameters used in the model, new generation capacity of type k can be added to bus b at a capital cost $CI_{b,k}$ in $/MW/yr. Regarding RES investments, we assume that capital costs decrease by 5% every period t (i.e., every 5 years). RES plants are operated at a marginal cost $MC_{b,k}$ $/MWh. Capital cost of adding a new circuit to corridor l is CC_l. Parameter $Y^0_{b,k}$ is the existing generation capacity of type k at bus b; parameter $Y^M_{b,k}$ is the maximum generation capacity expansion of type k allowed at bus b, and parameter $W_{b,k,h,t}$ is the capacity factor of generation of type k at bus b and hour h. Line capacities and susceptances are represented by parameters $F_{l,c}$ and $\gamma_{l,c}$, respectively.

Energy demand at bus b and hour h in year t is denoted as $D_{b,h,t}$. Demand increases over the years by the percentages determined in the demand forecasting study published by the Chilean National Energy Commission, based on 2016 demand. The RES quota requirement is $\alpha = 0.2$, expressed as a fraction of the supplied energy. To avoid unrealistic results, we consider a capacity expansion limit for each generation technology, per period. This capacity expansion limit, denoted by $IL_{t,k}$, differs among technologies.

Logical relationships are added to the constraint set so that generation and transmission capacities constructed in one year are also available in later years. Any specific transmission line can only be constructed once. The discount rate is δ.

5. Data for model implementation

Information about transmission lines currently used in Chile, as well as the transmission lines that are in process of construction, and those that have construction approval, but have not begun to be built were taken from CDEC-SIC (2017), CDEC-SING (2017), CNE (2016a), and CNE (2016b). For every transmission line, we obtained its maximum power flow capacity (in MW) and its reactance. Information about currently installed capacity of coal, diesel, natural gas, wind power, run-of-river hydro, reservoir hydro, and solar power plants in every zone, by type of generation technology, was also obtained from CDEC-SIC (2017) and CDEC-SING (2017).[7]

We use the hourly expected generation obtained in Section 3 for computing the initial (2016) capacity factor of wind farms (generation was measured every hour of the day and then it was compared to the maximum capacity of every power plant, calculating the factor capacity that every power plant had in a specific time block and on a specific day of the month). In every period (i.e., every five years) between 2016 and 2101, we incorporate changes in energy demand and in wind plant capacity factors. For each of these 18 5-year periods, we analyze the twelve representative days obtained through the k-means clustering technique, as explained in Section 3. The discount rate assumed in this study is 2.715%. This discount rate corresponds to the average inflation rate in Chile during 2016.

The initially installed power capacity in year 2016 in Chile is presented in Fig. 8 (amounts in MW). Wind represents only 6% of total power capacity. The sum of coal, diesel and natural gas power capacity is 57%. The Chilean Minister of Energy pursues the challenge of increasing the proportion of RES supply up to 70% by 2035, which may highlight the role of wind power in the future (Ministry of Energy, 2015, 2016).[8]

6. Simulation results

The model was implemented in a computational cluster composed of 21 computational nodes, each one with an Intel processor E5-2470,

[7] All data used in the Case Study implemented in this manuscript are publicly available in the cited sources. This information is also available upon request to crosende1@uc.cl

[8] Ministerio de Energía. "Energía 2050 Política Energética Chile". http://www.energia.gob.cl/sites/default/files/energia_2050_-_resumen_de_la_politica_energetica_de_chile.pdf.

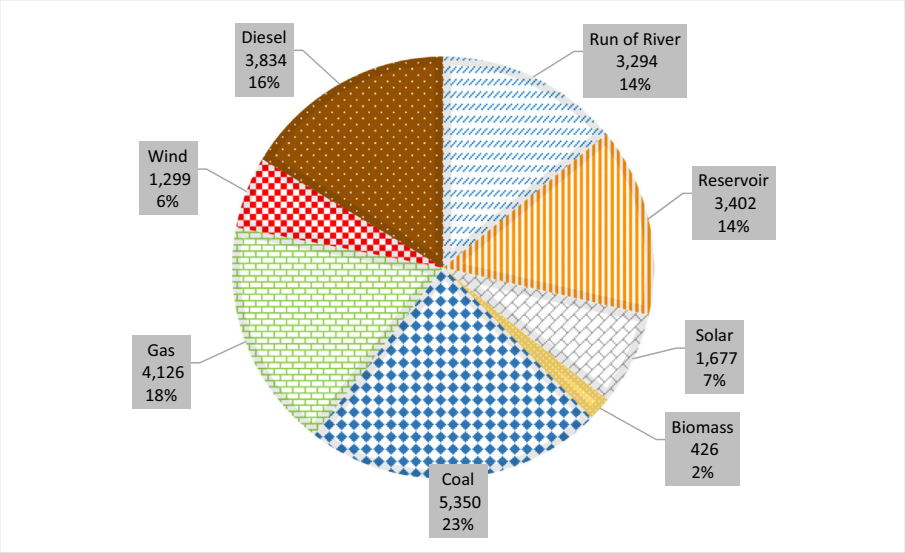

Fig. 8. Power capacity (in MW) installed in Chile, in 2016.

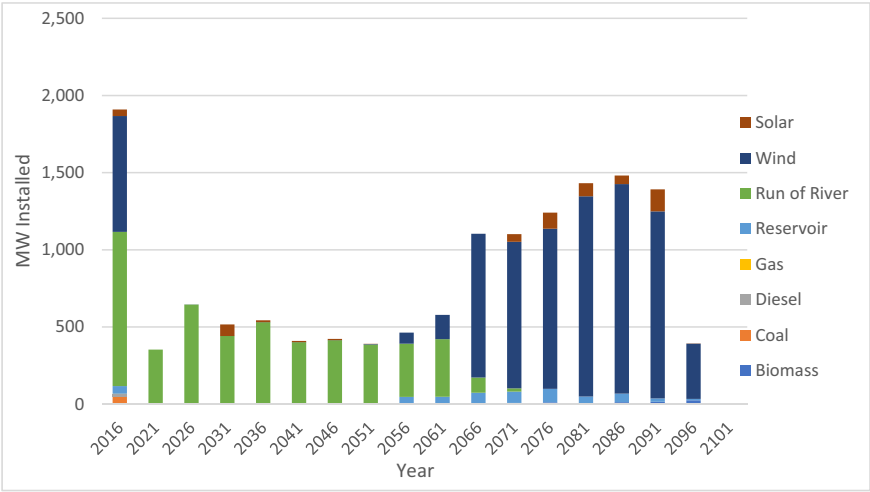

Fig. 9. Case 1: Power capacity expansion (in MW) considering the impact of Climate Change on wind.

8 Cores, 2.3 GHz, 32 GB RAM, and 50GB SSD of hard disk. The results are described in the next subsections.

6.1. Main results

The model yields the following results (see Figs. 9 and 10) for Case 1, which assumes that Climate Change affects wind speeds and hence wind farm capacity factors. Fig. 9 displays the optimal capacity expansion determined by the model in every period, under this scenario. There is a strong predominance of wind and run-of-river capacity expansion.[9] Fig. 9 clearly shows that run-of-river capacity investments are made mainly at the beginning of the planning horizon (for economic reasons) and wind capacity additions are preferably made after the available run-of-river capacity is already installed.

As exhibited in Fig. 10, of the total power capacity installed throughout the 85-year period, 56% corresponds to capacity installed in wind energy (8126 MW), 35% to capacity installed in run-of-river hydro (5000 MW), 4% to solar power capacity (587 MW), and 4% to reservoir hydro power capacity (502 MW). It is worth to mention that the generation capacity expansion limit is reached for the run-of-river hydro technology before the end of the 85-year period.

Regarding transmission lines, results show that, in Case 1, it is cost-efficient to invest, during the first period analyzed, in seven lines. The next cost-efficient investment in transmission lines is in year 2046, installing one additional line.

Case 2 assumes that wind capacity factors remain constant at their 2016 level (i.e., data is not adjusted with projections of effects of Climate Change on wind speeds). Fig. 11 exhibits optimal capacity expansion for every period. The total capacity expansion between 2016 and 2101 is shown in Fig. 12. Again, there is a predominance of capacity expansion in wind (56%) and run-of-river hydro (36%). Comparing these outcomes with the previous ones, it is noteworthy that total capacity expansion is lower by 331 MW when we assume constant wind capacity factors. The main driver for this is the lower investment in wind power capacity

[9] Although we consider annualized investment costs to avoid end-of-horizon distortions, there is a small capacity expansion in the last period. The reason for this is that several cheap-generation technologies already reached the capacity expansion limits in some periods before 2100, so the system gets lack of cheap-energy expansion alternatives in the last period.

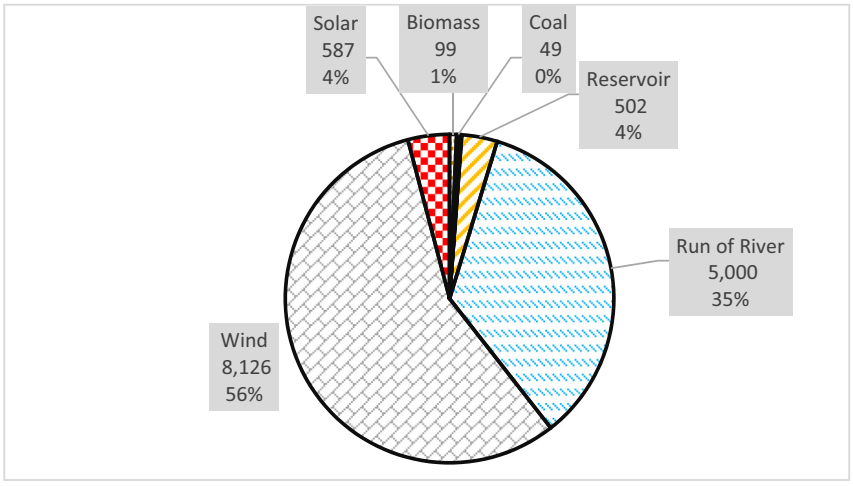

Fig. 10. Total power capacity expansion (in MW) in 2016–2101, in Case 1.

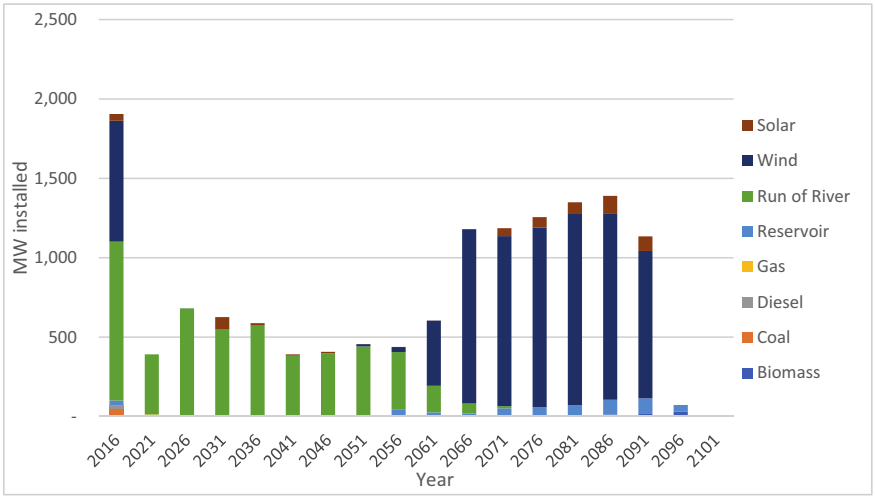

Fig. 11. Case 2: Power capacity expansion (in MW) considering constant capacity factors on wind power plants.

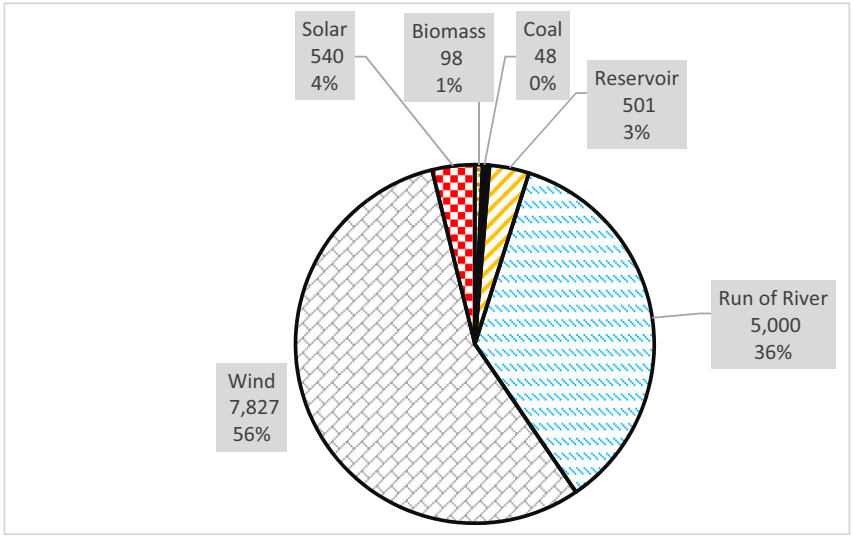

Fig. 12. Total power capacity expansion (in MW) in 2016–2101, in Case 2.

Table 1
Power capacity expansion by type of technology in the period 2016–2101 (in MW).

	Case 1: Considering impact of Climate Change on wind	Case 2: Considering constant wind capacity factors	Difference between expansions (MW)
Biomass	99	98	1
Coal	49	48	1
Diesel	18	21	(3)
Natural gas	4	19	(15)
Reservoir	502	501	1
Run of river	5000	5000	–
Wind	8126	7827	299
Solar	587	540	47
Total	14,385	14,054	331

when we assume constant wind capacity factors (i.e., 7827 MW in new wind power capacity in Case 2 instead of the 8126 MW in Case 1). That is, by ignoring the potential effects of Climate Change on wind speeds, we roughly underestimate wind power production and, consequently, the model optimally decides to install less capacity in wind power plants.

Table 1 compares the new installed generation capacity in both cases. It is interesting to note that changes in wind speeds affect not only capacity expansion in wind power capacity, but also capacity expansion in other power generation technologies. In Case 2, results suggest larger capacity expansion in natural gas and diesel; and lower capacity expansion in solar power, than Case 1. When influence of Climate Change on wind speed is taken into account (Case 1), results suggest installing 71 MW in coal, natural gas, and diesel (taken together); while capacity expansion in coal, natural gas, and diesel is 88 MW in Case 2. The sum of the capacity installed between 2016 and 2101 in wind power generation, run-of-river hydro, and solar plants is 13,713 MW in Case 1, and 13,367 MW in Case 2. However, only 299 MW corresponds to lower capacity installed in wind plants; while the rest of the difference between Case 1 and Case 2 is mainly due to the capacity expansion difference in solar power.

When comparing both cases regarding the capacity installed, the reader must bear in mind that capacity expansion limits were imposed on all technologies. Accordingly, the run-of-river hydro technology reached the generation capacity expansion limit before the end of the 85-year horizon in both cases, leading to the 5000 MW of new installed capacity. Unconstrained optimization might have different (although unrealistic, for the Chilean case) results.

Due to the magnitude of the problem, we optimized the model with 0.01% optimality gap. Hence, relatively small differences between both cases -like those that appear in Table 1 for biomass, coal, and reservoir hydro power- may be partly explained by the optimality gap chosen.

6.2. Sensitivity analyses

6.2.1. Relaxing some capacity expansion limit assumptions

The performed studies assumed a capacity expansion limit for each one of the generation technologies, for every 5-year period. The capacity expansion limit imposed on run-of-river hydro is reached before the end of the 85-year horizon in both cases analyzed in the previous section. Accordingly, it results interesting to study the changes in the model outcomes if the capacity expansion limit assumptions were less restrictive. In particular, in this section, we analyze how capacity expansion in wind technology would be affected when allowing a more accelerated investment process in the run-of-river hydro technology.

For run-of-river hydro, we had assumed a 5-year period capacity expansion limit of 1000 MW, in the whole system. In this section, we analyze the effect of increasing by 500 MW this limit. In addition to that, we also include a constraint ensuring that the total run-of-river capacity added during the entire planning horizon is less or equal than the 5000 MW installed in the previous-section cases. This is done in order to analyze the effects of allowing a more accelerated investment process in the run-of-river hydro technology, but still ensuring a realistic amount of total investments in this technology according to the physical characteristics of the Chilean power system.

In Case 1, which takes into account the impact of Climate Change on wind, results of the sensitivity analysis suggest that 56% of the installed capacity corresponds to wind power plants (8122 MW); 35% to run-of-river hydro (5000 MW); 4% to solar power plants (589 MW); and 4% to reservoir hydro plants (513 MW). Fig. 13 shows the total power capacity installed from 2016 to 2101, in the various types of generation technologies, when capacity expansion limits in run-of-river hydro are expanded by 500 MW per period and the impact of Climate Change on wind is taken into account.

In Case 2, which assumes no effect of Climate Change on wind speeds, increasing the per-period capacity expansion limits for run-of-

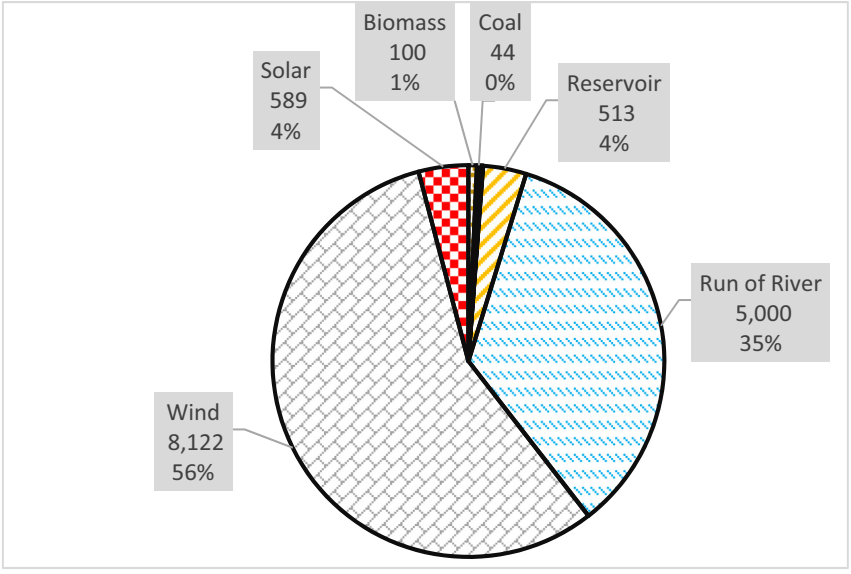

Fig. 13. Total power capacity expansion (in MW) in 2016–2101, in Case 1, when run-of-river hydro power capacity is available sooner.

Table 2
Power capacity expansion by type of technology in the period 2016–2101 (in MW) if capacity expansion limit for run-of-river hydro is expanded by 500 MW.

	Case 1: Considering impact of Climate Change on wind	Case 2: Considering constant wind capacity factors	Difference between expansions (MW)
Biomass	100	97	3
Coal	44	48	(4)
Diesel	25	36	(11)
Natural gas	3	15	(12)
Reservoir	513	498	15
Run of river	5000	5000	–
Wind	8122	7853	269
Solar	589	534	55
Total	14,396	14,081	315

river hydro yields model outcomes that suggest that 56% of the installed capacity corresponds to wind power plants (7853 MW); 35% to run-of-river hydro (5000 MW); 4% to solar power plants (534 MW); and 4% to reservoir hydro plants (498 MW). In Case 2, total capacity installed is 315 MW less than in Case 1. Table 2 summarizes the results of the sensitivity analysis, showing that if the impact of Climate Change on wind speed is taken into account, capacity expansion in wind, solar, and reservoir hydro technologies is larger (in MW) than if wind capacity factors are considered constant. In this particular sensitivity analysis, wind capacity installed decreases by 269 MW if wind capacity factors are considered constant. This is smaller than the 299 MW wind capacity expansion difference between Case 1 and Case 2 reported in Table 1. An explanation for this is that the acceleration of run-of-river capacity investments leads to the need of relatively more capacity investments in other technologies in the first half of the planning horizon, making, on the one hand, wind capacity additions a little less attractive than before if we consider the effects of Climate Change on wind speeds (because, as explained in Section 3, Climate Change would likely increase wind speeds toward the end of the planning horizon) and, on the other hand, wind capacity additions more attractive than before if we ignore those effects on wind speeds. Therefore, in a situation of less constrained capacity expansion in run-of-river hydro, a higher variability in wind speeds (Case 1) will result in less capacity expansion in wind power and more capacity expansion in other technologies than in the cases reported in Table 1.

6.2.2. Increasing the discount rate to 6%

The discount rate assumed before was 2.715%. We now analyze what would happen with the capacity expansion if the project discount rate were 6%, the rate that has been used to discount several energy (social) projects for Chile (CORFO, Oct. 2013; NRDC and ACERA, 2013). Again, we run the model for Case 1 (changing wind capacity factors) and Case 2 (constant wind capacity factors).

Fig. 14 exhibits the results for Case 1. The larger discount rate naturally causes some investments to be postponed, but the sum of capacity installed by 2101 - in terms of MW per technology- is relatively similar to that using the original discount rate. In particular, comparing Figs. 9 and 14, we observe that most of the wind power investment made in the first period (2016) is postponed when using a higher discount rate (and replaced, in that first year, by investments in run-of-river hydro, coal, and diesel technologies). Wind power investments in the second half of the planning horizon are also postponed when using a higher discount rate, but this difference is less significant than in the first period due to the long planning horizon considered. The rationale of these differences is that wind power investments are more capital intensive than investments in other technologies, implying that a higher discount rate leads to postponing capital-intensive technology investments (e.g., wind power investments) and accelerating low-capital technology investments (e.g., run-of-river hydro, coal, and diesel investments).

Fig. 15 shows that, summing up all the capacity installed in all the periods, results are: 7453 MW installed in wind power (54%), 5000 MW in run-of-river hydro (37%), 529 MW in solar power (4%), and 489 MW in reservoir hydropower (4%).

In Case 2 (constant wind capacity factors), increasing the discount rate to 6% results in a decrease in the total capacity installed of 568 MW, in comparison to Case 1. In this case, 51% of the total capacity installed is in wind power (6665 MW), 38% in run-of-river hydro (5000 MW), 5% in solar power (660 MW), and 5% in reservoir hydropower (605 MW). Table 3 compares both cases for a 6% discount rate. Similarly to previous comparisons, if wind capacity factors are constant, the capacity installed is lower (than when considering variable wind capacity factors) for wind, biomass, and coal technologies, and higher (than when considering variable wind capacity factors) for solar, reservoir hydro, and natural gas technologies, when using a 6% discount rate.

7. Discussion and conclusions

After concluding that, in Chile, there are no high correlations between the hourly power generation by wind plants and by other RES technologies, we studied wind speed projections (from the National Center for Atmospheric Research database) under three scenarios of concentration of greenhouse gases, concluding that –due to Climate

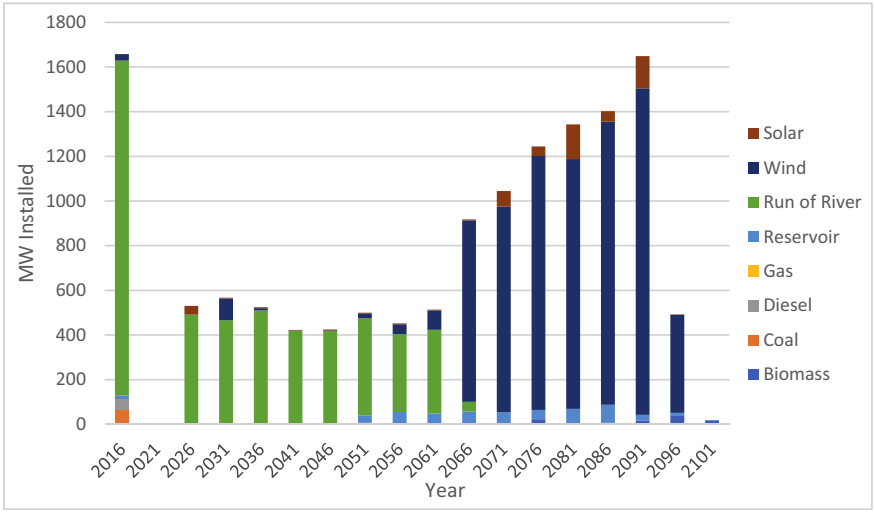

Fig. 14. Power capacity expansion (in MW) considering a discount rate of 6%, in Case 1.

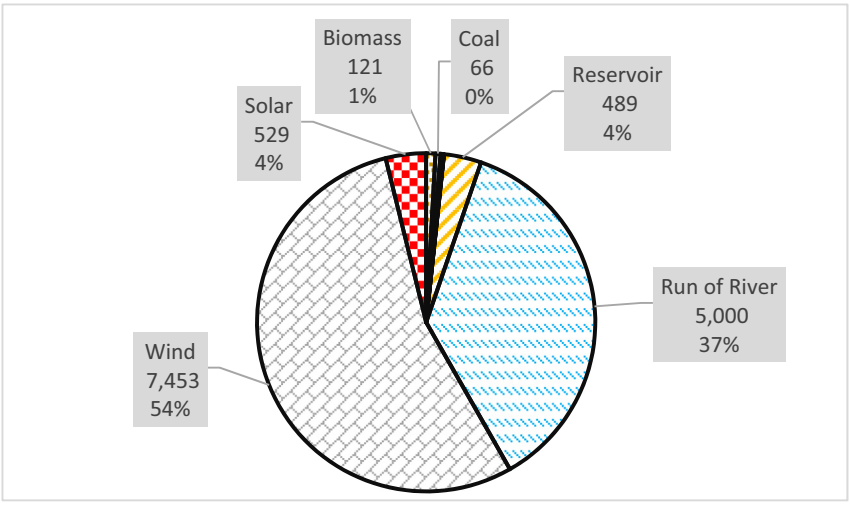

Fig. 15. Total power capacity expansion (in MW) in 2016–2101, in Case 1, considering a discount rate of 6%.

Change- wind speeds in Chile will, on average, become slightly more intense, but will also have greater variability. In some nodes in the northern and southern parts of Chile, wind speeds are likely to increase significantly, making wind energy generation more cost-effective. These facts motivated the analysis of the optimal power capacity expansions for the Chilean power matrix (2016–2101) in the case Climate Change affects wind speeds (Case 1), and then comparing those results with the optimal power capacity expansions in the case wind capacity factors remain unaltered (Case 2).

To do so, we formulated and implemented an optimization model that co-optimizes transmission and generation capacity expansion among power technologies, nodes, and years in order to minimize total system costs, while satisfying the increasing demand and fulfilling the national regulations regarding the percentage of generation that must come from RES.

The findings are significant: if Climate Change affects wind capacity factors, the sum of power capacity installed between 2016 and 2101 are 331 MW higher than if wind capacity factors remain constant. Power capacity expansion in diesel and natural gas is relatively lower, and capacity expansion in wind and solar power relatively higher in Case 1 than in Case 2.

The sum of the capacity installed between 2016 and 2101 in wind power generation, run-of-river hydro, and solar plants is 13,713 MW in Case 1 and 13,367 MW in Case 2. However, only 299 MW corresponds to lower capacity installed in wind plants; while the rest of the difference between Case 1 and Case 2 is mainly due to the capacity expansion difference in solar power.

Results are robust to changes in capacity expansion limits and changes in the discount rate. When allowing a more accelerated investment process in the run-of-river hydro technology (but still ensuring a realistic amount of total investments in this technology), we found that a higher variability in wind speeds (Case 1) will result in less capacity expansion in wind power and more capacity expansion in other technologies than in the situation of more constrained capacity expansion in run-of-river hydro. An explanation for this is that the acceleration of run-of-river capacity investments leads to the need of relatively more capacity investments in other technologies in the first half of the planning horizon, making, on the one hand, wind capacity additions a little less attractive than before if we consider the effects of Climate Change on wind speeds (because Climate Change would likely increase wind speeds toward the end of the planning horizon) and, on the other hand, wind capacity additions more attractive than before if we ignore those effects on wind speeds.

A larger discount rate causes some investments to be postponed. In particular, we observe that most of the wind power investment made in the first period is postponed when using a higher discount rate (and replaced, in that first year, by investments in run-of-river hydro, coal, and diesel technologies). This occurs because wind power investments are more capital intensive than investments in other technologies, implying that a higher discount rate leads to postponing capital-intensive technology investments (e.g., wind power investments) and accelerating low-capital technology investments (e.g., run-of-river hydro, coal, and diesel investments).

The methodology implemented has also some shortcomings. The main shortcoming is the use of a limited number of time steps to characterize wind variation. The more representative days are selected for the wind variation characterization, the more we capture the variations of wind through the year. However, we were not able to get a satisfactory model solution when employing a large number of representative days per year in the simulations. We left as future work the study of some variance-reduction techniques to allow the consideration of more representative days per year to characterize wind variation.

This study provides optimal power capacity expansion projections, showing the increasing importance that RES will have in Chile in the next 85 years, particularly considering the effect of Climate Change on wind speeds. The share of wind in the Chilean power matrix will augment, reaching 56% in year 2101. Overall, the Chilean matrix will become more environmentally friendly.

Table 3
Power capacity expansions by type of technology in the period 2016–2101 (in MW) in the case of considering a discount rate of 6%.

	Case 1: Considering impact of Climate Change on wind	Case 2: Considering constant wind capacity factors	Difference between expansions (MW) (Case 1–Case 2)
Biomass	121	103	18
Coal	66	51	15
Diesel	42	41	1
Natural gas	2	9	(7)
Reservoir	489	605	(116)
Run of river	5000	5000	–
Wind	7453	6665	788
Solar	529	660	(131)
Total	13,702	13,134	568

Acknowledgments

The research reported in this work was partially supported by the CONICYT, FONDECYT/Regular 1161112 grant and by CONICYT, FONDAP 15110019 grant (SERC-CHILE).

References

Barton, J., 2013. Climate change adaptive capacity in Santiago de Chile: creating a governance regime for sustainability planning. Int. J. Urban Reg. Res. 37 (6), 1916–1933.

CDEC-SIC, 2015. Demand Forecast Study 2015–2035 (Estudio de Previsión de Demanda 2015–2035). https://sic.coordinadorelectrico.cl/wp-content/uploads/2015/06/Informe-Final-Estudio-de-Previsi%C3%B3n-de-Demanda-2015.pdf.

CDEC-SIC, 2017. Real Operation – CDEC SIC (Operación Real - CDEC SIC). Retrieved February 3, 2017, from https://sic.coordinadorelectrico.cl/informes-y-documentos/fichas/operacion-real/.

CDEC-SING, 2017. Real Operation – CDEC SING (Operación Real - CDEC SING). Retrieved February 3, 2017, from http://cdec2.cdec-sing.cl/pls/portal/cdec.pck_web_coord_elec.sp_pagina?p_id=5193.

Chilean National Energy Commission, CNE, 2016a. 2016 Annual Statistics of Energy (Anuario Estadístico de Energía 2016). Santiago, Chile. Retrieved from http://www.energia.gob.cl/sites/default/files/anuariocne2016final3.pdf.

Chilean National Energy Commission, CNE, 2016b. Generation and Transmission Expansion Plan of the Central Interconnected System and the Northern Interconnected System (Programa de obras de generación y transmisión del Sistema Interconectado Central y del Sistema Interconectado del Norte Grande). Santiago. Retrieved from https://www.cne.cl/wp-content/uploads/2016/08/Informe-Programa-de-Obras-Agosto-2016.pdf.

CORFO, 2013. Renewable Energy: Available Types and Applications to Agriculture (Energías Renovables: Tipos Disponibles y Aplicaciones en la Agricultura). http://www.cnr.gob.cl/FomentoAlRiego/Documentos%20Difusin%202013/Presentaciones%20Taller%20ERNC/CNR_ERNC_2013%20Presentaci%C3%B3n%20CER.pdf.

Cradden, L., Harrison, G., Chick, J., 2012. Will climate change impact on wind power development in the UK? Climate Change 115, 837–852.

Dirección meteorológica de Chile - Subdepartamento de climatología y meteorología aplicada (DGAC Chile), 2016. Climate Report (Reporte Climático). http://archivos.meteochile.gob.cl/portaldmc/meteochile/documentos/reporteanual2016.pdf.

Garreaud, Rene, 2011. Cambio climático: bases físicas e impactos en Chile. Revista Tierra Adentro. INIA, No. 93. http://dgf.uchile.cl/rene/PUBS/inia_RGS_final.pdf.

Garreaud, R., Falvey, M., 2008. The coastal winds off western subtropical South America in future climate scenarios. Int. J. Climatol. 29 (4), 543–554. http://dgf.uchile.cl/rene/PUBS/future_coastal_winds_IJCL.pdf.

Harrison, G.P., Cradden, L.C., Chick, J.P., 2008. Preliminary assessment of climate change impacts on the UK onshore wind energy resource. Energy Sources, Part A 30 (14–15), 1286–1299.

IPCC Intergovernmental Panel on Climate Change, 2000. IPCC Special Report. Emissions Scenarios. Summary for Policymakers. https://www.ipcc.ch/pdf/special-reports/spm/sres-en.pdf.

IPCC Intergovernmental Panel on Climate Change, 2013. Fifth Assessment Report. http://www.ipcc.ch/report/ar5/wg2/.

Ministry of Energy, 2015. Energy 2050: Chilean Energy Policy. http://www.energia.gob.cl/sites/default/files/energia_2050_resumen_de_la_politica_energetica_de_chile.pdf.

Ministry of Energy, 2016. CIFES Report. Renewable Energy in the Chilean Power Market (Reporte CIFES. Energías renovables en el mercado eléctrico chileno) Comité Corfo. Ministerio de Energía. Gobierno de Chile.

Mundaca, L., 2012. Climate change and energy policy in Chile: up in smoke? Energy Policy 52, 235–248.

Munoz, F., Sauma, E., Hobbs, B., 2013. Approximations in power transmission planning: implications for the cost and performance of renewable portfolio standards. J. Regul. Econ. 43 (3), 305–338.

Munoz, F., Pumarino, B., Salas, I., 2017. Aiming low and achieving it: a long-term analysis of a renewable policy in Chile. Energy Econ. 65, 304–314.

NCAR, 2017. National Center for Atmospheric Research NCAR UCAR. https://ncar.ucar.edu/about-ncar.

NRDC and ACERA, 2013. Economic benefits of the non-conventional renewable energy in Chile (Beneficios Económicos de Energías Renovables No Convencionales en Chile). Natural Resources Defense Council and Asociacion Chilena de Energías Renovables. http://www.acera.cl/wp-content/uploads/2016/09/11.2013-Beneficios-Economicos-ERNC.pdf.

Sailor, D.J., Smith, M., Hart, M., 2008. Climate change implications for wind power resources in the North West. Renew. Energy 33, 2393–2406.

Santana, C., 2014. Energías renovables en Chile: El potencial eólico, solar e hidroeléctrico de Arica a Chiloé. Proyecto Estrategia de Expansión de las Energías Renovables en los sistemas eléctricos interconectados.

Staffell, I., Pfenninger, S., 2016. Using bias-corrected reanalysis to simulate current and future wind power output. Energy 114, 1224–1239. http://www.sciencedirect.com/science/article/pii/S0360544216311811.

Watts, D., Jara, D., 2010. Statistical analysis of wind energy in Chile. Renew. Energy 36, 1603–1613.

Watts, D., Oses, N., Perez, R., 2016. Assessment of wind energy potential in Chile: a project-based regional wind supply function approach. Renew. Energy 96, 738–755.